

Retraction

Retracted: Simulation Study on the Spatiotemporal Difference of Complex Neurodynamics between P3a and P3b

Complexity

Received 23 January 2024; Accepted 23 January 2024; Published 24 January 2024

Copyright © 2024 Complexity. This is an open access article distributed under the Creative Commons Attribution License, which permits unrestricted use, distribution, and reproduction in any medium, provided the original work is properly cited.

This article has been retracted by Hindawi following an investigation undertaken by the publisher [1]. This investigation has uncovered evidence of one or more of the following indicators of systematic manipulation of the publication process:

- (1) Discrepancies in scope
- (2) Discrepancies in the description of the research reported
- (3) Discrepancies between the availability of data and the research described
- (4) Inappropriate citations
- (5) Incoherent, meaningless and/or irrelevant content included in the article
- (6) Manipulated or compromised peer review

The presence of these indicators undermines our confidence in the integrity of the article's content and we cannot, therefore, vouch for its reliability. Please note that this notice is intended solely to alert readers that the content of this article is unreliable. We have not investigated whether authors were aware of or involved in the systematic manipulation of the publication process.

In addition, our investigation has also shown that one or more of the following human-subject reporting requirements has not been met in this article: ethical approval by an Institutional Review Board (IRB) committee or equivalent, patient/participant consent to participate, and/or agreement to publish patient/participant details (where relevant).

Wiley and Hindawi regrets that the usual quality checks did not identify these issues before publication and have since put additional measures in place to safeguard research integrity.

We wish to credit our own Research Integrity and Research Publishing teams and anonymous and named external researchers and research integrity experts for contributing to this investigation.

The corresponding author, as the representative of all authors, has been given the opportunity to register their agreement or disagreement to this retraction. We have kept a record of any response received.

References

- [1] X. Wei, X. Ni, J. Liu et al., "Simulation Study on the Spatiotemporal Difference of Complex Neurodynamics between P3a and P3b," *Complexity*, vol. 2020, Article ID 2796809, 11 pages, 2020.

Research Article

Simulation Study on the Spatiotemporal Difference of Complex Neurodynamics between P3a and P3b

Xin Wei,¹ Xiaoli Ni ,¹ Junye Liu,² Haiyang Lang,² Rui Zhao,³ Tian Dai,³ Wei Qin,³ Wei Jia,⁴ and Peng Fang⁵

¹Institute of Social Psychology, School of Humanities and Social Sciences, Xi'an Jiaotong University, Xi'an 710049, China

²Teaching and Research Section of Radiation Medicine, Department of Military Preventive Medicine, The Fourth Military Medical University, Xi'an, China

³Sleep and Neuroimage Group, School of Life Sciences and Technology, Xidian University, Xi'an 710126, China

⁴Xi'an Gaoxin No. 2 Middle School, Xi'an 710119, China

⁵Department of Military Medical Psychology, Air Force Medical University, Xian 710032, China

Correspondence should be addressed to Xiaoli Ni; nixiaoli@xjtu.edu.cn

Received 27 March 2020; Revised 1 June 2020; Accepted 22 June 2020; Published 24 December 2020

Guest Editor: Zhihan Lv

Copyright © 2020 Xin Wei et al. This is an open access article distributed under the Creative Commons Attribution License, which permits unrestricted use, distribution, and reproduction in any medium, provided the original work is properly cited.

The integration of event-related potential (ERP) and functional magnetic resonance imaging (fMRI) helps to obtain and study neural networks with high temporal and spatial resolution. EEG/fMRI data proves that in the visual tritestimulus oddball paradigm, two P300 potentials (P3a and P3b) induced by target stimulation and novel stimulation are detected at the frontal-middle (Fz), center (Cz), and mid-apical (Pz) electrodes. Previous studies have shown that P3a and P3b have different spatial distributions of brain activation, but it is unclear whether they have the same neural mechanism. The purpose of this study is to determine the neuropsychological mechanisms of P3a and P3b, as well as the spatiotemporal differences in neurodynamics between the two ERP subcomponents. In a group of 25 subjects, P300 ERP induced by target stimulation and novel stimulation can be detected at the Fz, Cz, and Pz electrodes. At Cz and Fz, compared with P3b related to the target stimulus, the P3a related to the novel stimulus has a higher amplitude and the waveform declines more slowly. But at Pz, P3b has a higher amplitude than P3a. P3a appeared earlier than P3b at Cz and Fz, but the opposite phenomenon was observed at the Pz electrode. The activated brain regions of P3a included the left frontal-parietal lobe region, left anterior wedge lobe region, and right insula, while the target-driven P3b was significantly associated with BOLD changes in the bilateral fusiform gyrus, the left frontal region, and the bilateral insula. The results showed that the integration of the spatial and temporal information of the two imaging modes, namely, ERP and fMRI, proves the existence of the different brain function processes of the two P300 subcomponents. Through the analysis of the composition of P300, the results further proved that the top-down and bottom-up processing processes have played a role in the occurrence of attention capture. It is just that the modulation effects of the two processing mechanisms are different in different tasks. Therefore, it should be noted that the captured neural mechanism is not a single top-down or bottom-up processing process but should be the result of the interaction between the two.

1. Introduction

For the human, rapidly distinguishing the relevant targets from distracting stimuli is one of the critical ability to execute an appropriate response according to the environmental requirement. One widely used task to assess this cognitive ability is oddball paradigms. In a three-stimulus oddball, it presents infrequent target stimuli in a background

of frequent standard stimuli and infrequent novel stimuli, and the subject is instructed to respond mentally or physically to the target stimuli as quickly and accurately as possible, but not to others [1].

The brain activity related to this ability has been widely studied with electrical recordings using ERP. Previous ERP research has shown that the P300 is the characteristic endogenous positive wave, arising between 260 and 500 ms

after the onset of each rare stimulus, which is more prominent over the centroparietal region of the scalp [2]. The oddball tasks can typically evoke two highly characteristic P300 ERPs, the target-related P3b and the novel-related P3a. The P3b is seen as a long positive slow wave occurring after a button press, which is affected by the expected versus actual action effects [3]. And the scalp distribution is defined as the amplitude change over the three midline electrodes (Fz, Cz, and Pz), which typically increases from the frontal to parietal sites and is the largest over parietal areas [4]. An infrequent novel stimulation, presented in a series of frequent standard stimuli without a target stimulation, can produce a positive-going waveform with a frontoparietal maximum amplitude distribution and relatively short peak latency and was dubbed the P3a to distinguish it from the target-related P3b potential [5, 6]. Many studies have found that P3a and P3b have different topographic amplitude distributions and peak latency. P3a and P3b data, using a difficult target/standard discrimination task in a three-stimulus paradigm from 120 healthy young adults, have shown that P3a has a central maximum, whereas P3b has a parietal maximum, and the peak latency for both was shorter over the frontal and longer over the parietal sites [7]. The topographic variation suggested that there may be overlapping neural activation patterns, which are functionally distinct [8, 9].

However, EEG traceability positioning is a relatively complicated problem, and there are infinitely many solutions that satisfy the EEG signal recorded by the scalp. Therefore, we need a priori assumption to constrain the solution space to obtain a unique solution. Functional magnetic imaging (fMRI) can be used to study the source localization of P300; many studies have identified brain activation evoked by detecting targets and novels in oddball tasks, which have shown different neuronal networks activated by targets (right temporoparietal junction and inferior frontal gyrus) and by novels (intraparietal sulcus and left inferior frontal sulcus) [10–13]. The relationship between abnormal ERP components and dysfunctional fMRI activation during oddball tasks in patients has also been extensively studied. Patients with frontal lobe lesions demonstrated diminution of P3a amplitude, whereas the same patients demonstrated a parietal maximum for the P3b, which suggested that frontal lobe integrity is necessary for P3a generation [14]. For the patients with comorbid depressive and anxiety disorders, findings showed an abnormal frontal-greater-than-parietal P3b topography in the right hemisphere and the highest P3a amplitude at frontal and central sites at the scalp midline [15]. It is proposed that P300 amplitude is affected by temporal-parietal junction integrity for its absence greatly reduces component size over the parietal area [16, 17]. This connection implies that the P3a and P3b indicate a circuit pathway between frontal and temporal/parietal brain areas [18, 19].

Event-related potential (ERP) and functional magnetic resonance (fMRI) are two advanced functional detection techniques for nondamaging brains today. EEG signal is a biological electrical activity spontaneously generated by the central nervous system, contains a wealth of information on

the state and changes of the nervous system, and can reflect the brain's skin reflection on stimulation. EEG signals are easier to obtain, and it is easier to establish interfaces with external devices (such as computers) to achieve direct interaction between the human brain and computers. This interaction is realized through brain-computer interface technology and then realizes a system to control the brain. EEG/ERP has a high temporal resolution and can track the processing of brain information, but the spatial resolution is low. fMRI can repeatedly observe and study the human brain function (language, cognition, exercise, etc.). It can not only observe the structure and shape of the brain but also get real-time information about blood flow functional images and metabolism. However, fMRI has a high spatial resolution, but a low temporal resolution. Combining EEG and fMRI signals and using information fusion theory to find the relationship between them may become a new and very effective method for scientific analysis and processing of brain function data.

Brain function modeling has always been a big problem that puzzled scholars from various countries. Due to the complexity of brain structure and function, it is difficult to model brain function alone. Internationally, the research on brain function modeling in recent years has mainly focused on the detection of EEG and fMRI signals. In order to improve the sensitivity and accuracy of detection, foreign researchers in recent years have vigorously improved measurement equipment and measurement methods; for example, improving the field strength of fMRI is very high. And some new methods in the extraction of useful signals and noise filtering, feature extraction, and data classification improve the signal quality of EEG and fMRI and the effectiveness of feature extraction, but this progress is slow. A new trend is that brain function detection is developing in conjunction with multiple technologies. For example, MRI and PET use image fusion or registration technology to obtain more information on brain functional activities; at the same time, EEG and MRI signals are obtained for information fusion can get more comprehensive features of brain function and improve resolution. Research in this area has been carried out in Germany, Canada, Japan, and other countries and a few domestic units. The representative of the Charlotte Hospital in Germany scans fMRI images while acquiring EEG signals for pathological research and pattern recognition and localization of brain function when the brain receives different stimuli from the body. But their research has just begun, and the correlation between EEG and fMRI signals is lacking.

Obtaining high imaging resolution and correct interpretation, analysis and processing of brain activity features have become the frontier of current research. The use of brain functional imaging technology to model, classify, and recognize the pattern of human brain nerve response can not only provide a more accurate and rich basis for the diagnosis of certain diseases but also more objectively study the human brain in psychology and intelligence. This aspect of the activity lays the foundation and is a crucial step in further understanding the function of the brain and the connections between the peripheral nerves and the brain. Due to the high

cost and difficulty of using a single method to improve resolution and improve the analysis of brain functional characteristics, and the fact that any single method has its own advantages and disadvantages, no modern medical imaging technology is perfect and can be suitable for all experiments or clinical applications. It is precisely because of the incompleteness of a single imaging method that more and more researchers begin to consider the fusion of multiple modalities of medical images, so it is an effective technical approach to use multiple technical means to obtain composite signals and perform information fusion.

In the present simultaneous ERP/fMRI experiment, 25 healthy participants were confronted with a visual three-stimulus oddball (standard, target, and novel stimuli). The present study aimed to explore the differences of the spatiotemporal neural dynamics between the P3a and P3b and the neuropsychological origins underlying these two ERPs.

The main purpose of this study is to accurately locate the brain activation status of the target recognition process. One of the methods is to use the EEG data collected by the scalp to calculate the activation status in the brain. However, due to the low spatial resolution of the EEG data, the EEG accurate calculation of dipole data also requires certain assumptions, so it is very difficult to accurately obtain the position of the brain source. With the development of modern brain imaging technology, especially the application of functional magnetic resonance technology, it has made an accurate determination of brain activity and location becomes possible. The spatial resolution of functional magnetic resonance technology is very high, but the temporal resolution is limited. In order to further study the brain activation of P300 operation, we combined high-resolution EEG with high-spatial-resolution functional magnetic resonance technology in this process.

To show the novelty of our research, in fMRI acquisition and analysis, we added combined ERP/fMRI analyses to test for significant BOLD changes of each deviant stimulus (target, novel) with covariates defined using the P300 amplitude or latency. Given that both P300 amplitude and latency are informative to analyze the fMRI data, which suggest that measures of ERPs' amplitude may reflect the intensity of responses whereas measures of latency may reflect time duration of responses [20, 21], therefore, we used these two parameters as covariates to constrain fMRI data in the General Linear Model. In this way, we have found other forms of specific brain activation associated with P3a and P3b, such as hippocampal gyrus, bilateral fusiform gyrus, and insula, which extends prior studies.

The mainstream view is that selective attention is controlled by the combined brain area of the parietal and frontal lobes (e.g., SPL of the parietal lobe, FEP of the frontal eye area, SEP of the auxiliary eye area, etc.), which is perceived through top-down neural connections analysis [22, 23]. However, recent studies on time orientation have shown that attention control and attention regulation involve several other different neural mechanisms. Some researchers believe that the neural mechanisms of temporal and spatial expectations are independent. Spatial expectations affect early perception components, such as P1 and starvation time

expectations, which affect the late selection or response-related components, such as P300 components [24, 25]. Other researchers believe that the neural mechanisms of temporal and spatial expectations are partially independent and partially overlapping. They also admit that spatial expectations affect early perception components, but they believe that, according to different mission requirements, temporal expectations affect different stages of stimulus processing, including the early perception stage and late response selection stage [26, 28]. Coull and Nobre [27] used functional nuclear magnetic resonance imaging (fMRI) technology to find that there is a partial overlap between the neural mechanisms of spatial and temporal attention toward the task. Spatial and temporal attention showed hemispherical asymmetric activation on the right and left parietal lobe, respectively. And when paying attention to both time and space information, both parietal lobes are activated.

2. Methods

2.1. Subjects. Twenty-five healthy volunteers (average age = 22 ± 3 years, range = 20–31 years, 22 men and 3 women), with no history of neurological or psychiatric diseases, participated in this study. All participants were carefully screened to ensure that they met the inclusion and exclusion criteria. They were all right-handed with normal or corrected to normal visual acuity. Finally, all participants provided written informed consent after the experimental procedures were fully explained.

2.2. Study Procedure. All participants completed the visual oddball task inside the scanner under a typical fMRI scanning environment with an MR-shielded EEG cap on. During this experiment, a visual three-stimulus oddball task was presented via the E-Prime software (Psychology Software Tools, Pittsburgh, USA). The novels were large colorful checkerboard squares (never repeated), and the targets were blue discs which were slightly larger than the standard blue discs. Within each task, a total of 128 stimuli were shown: 103 standard stimuli (85%), 15 target stimuli (12%), and 10 novel stimuli (8%). All stimuli were presented for 30 ms with an interstimulus interval of 1800 ms. All stimuli were in a pseudorandom sequence both within and between 25 subjects. Each participant laid inside the fMRI scanner with a button press box placed in the right hand, and they were instructed to press with their thumb when a larger blue disc was presented.

The radiology laboratory of Xijing Hospital uses a direct rear projection visual stimulation device. The projection system is completely nonmagnetic radio frequency shielding, which can be placed in the magnetic resonance scanning room and has an air-cooled heat dissipation device to ensure the stability of the projection. Compared with the general placement of projectors in the scanning control room, the rear projection method can avoid brightness attenuation and visual signal attenuation, maintain uniform brightness, ensure high-resolution visual signals, ensure the consistency of the experimental environment, and can easily be compared with others.

Magnetic resonance imaging brain functional audio visual stimulation system is mainly used in fMRI experiments to carry out visual and auditory stimulation. The system has good magnetic compatibility, can work normally in 3T MRI environment, and provides clear visual and auditory information to the subjects in the experimental process. According to the need, the experimenter can send the specific text, image, sound, and other experimental stimulus information materials to the subjects. At the same time, the feedback information of the subjects can be recorded in real time through key operation. There is also a clear voice communication between the experimenter and the subjects. The experimental stimulation task is synchronized with MRI scan, which ensures the time synchronization of brain function data and visual visual stimulation task. The system consists of visual stimulus host, data acquisition system, projection system, auditory stimulation module, stimulus feedback component, etc. (Figure 1).

The radiofrequency buttonless response control box designed according to ergonomics transmits the response of the subject directly to the computer through the CREATOR optical fiber transmission system. Event-related design can be used to statistically compare different types of cognitive tasks. CREATOR fiber optic synchronization system can send pulses to trigger the start of E-Prime stimulation program when the magnetic resonance scanning system starts scanning, so that the scanning and stimulation are strictly synchronized, providing a guarantee for accurate data analysis.

MRI examinations used the GE 3.0 T MRI scanner produced by the American General Medical Company and a 32-channel phased-array surface coil on the head. Conventional structural MRI examinations include T1W1 (TSE, TR/TE/TI 2510/9.6/1038 ms; flip angle 130°; layer thickness 3 mm; layer interval 0.3 mm; FOV 180 mm × 180 mm; matrix 256 × 256), T2WI (TSE, TR/TE 5000/93 ms, other scanning parameters are the same as before), and T2WI-FLAIR (TR/TE/TI = 9000/93/2500 ms; layer thickness 3.0 mm; layer interval 0.3 mm). In addition, in order to obtain a good gray-white contrast image, the scanning scheme also includes transversal IR sequence (TR/TE/TI = 1500/13/499 ms, layer thickness 4 mm, layer spacing 0.6 mm, flip angle 150°).

EEG data acquisition adopts 32-lead MR-compatible EEG system of German Brain Products company. The electrode is an antimagnetic material electrode. The electrode placement: the elastic electrode cap international 10–20 system is used to place the electrode. At the same time, the ECG is placed to record the heart rate change of the subject and identify electrocardiography traces. This study specifies that the scalp resistance is less than 10 k Ω and the acquisition frequency is 5000 Hz.

2.3. EEG Acquisition and Analysis. This laboratory uses a direct rear projection visual stimulation device. The projection system is completely nonmagnetic radio frequency shielding, which can be placed in the magnetic resonance scanning room, and there is an air-cooled heat dissipation device to ensure the stability of the projection. Compared with the general placement of projectors in the scanning control room, the rear projection method can avoid

brightness attenuation, visual signal attenuation, maintain uniform brightness, ensure high-resolution visual signals, ensure the consistency of the experimental environment, and can easily be compared with other The stimulation device is matched.

The CREATOR optical fiber synchronization system can send pulses to trigger the start of the E-Prime stimulation program when the magnetic resonance scanning system starts scanning, so that the scanning and stimulation are strictly synchronized, providing a guarantee for accurate data analysis.

The radiofrequency buttonless response control box designed according to ergonomics transmits the response of the subject directly to the computer through the CREATOR optical fiber transmission system. Event-related design can be used to statistically compare different types of cognitive tasks,

because it will generate a strong magnetic field when used in MRI work. According to the characteristics of magnetic resonance imaging (MRI), if the traditional VGA transmission cable is used, it will be interfered with by a large and strong magnetic field and cannot transmit signals normally. At the same time, the traditional VGA transmission cable will generate electrical and electromagnetic signals that will interfere with the normal operation of MRI. Therefore, CREATOR fiber transmission has become a wise choice. The biggest advantage of optical fiber transmission is the following. (1) It solves the long-distance or ultralong distance (tens of kilometers) VGA signal transmission and is the lossless transmission. (2) In many specific occasions, such as the electromagnetic environment, optical fiber transmission is very bad. The antijamming feature of the system can be brought into full play, expanding the range of VGA signal transmission applications. (3) Compared with the traditional analog cable mode, the thinking mode of all-digital and all-fibers is self-evident, and it will certainly bring a lot of new opportunities and growth points, which has been confirmed. (4) On many occasions, the comprehensive cost of digital fiber mode can be compared with analog and cable modes and may even be lower, which provides the possibility for a large number of future applications.

VGA signal transmission system uses CREATORVGA-F500 T/RVGA optical fiber transceiver, computer output, uses its VGA port to lead analog signals to VGA-F500TVGA optical fiber transceiver, and converts VGA signal to optical signal transmission. VGA-F500 R is responsible for optical revert to VGA signal. The signal quality after digital transmission can be greatly improved, and problems such as smearing, blurring, and ghosting, which were common in analog transmission in the past, will not occur.

Electroencephalogram (EEG) data was recorded simultaneously with fMRI data using a BrainAmp MR-compatible EEG system (BrainProducts GmbH, Munich, Germany), which includes a 32-channel MR-compatible amplifier and an MR-compatible EEG cap. The EEG cap included 30 scalp electrodes, one electrooculogram (EOG), and one electrocardiogram (ECG). The EOG electrode was placed beneath the subject's left eye to monitor the eye blink, and the ECG electrode was placed over the subject's back. The common recording reference was referenced online to

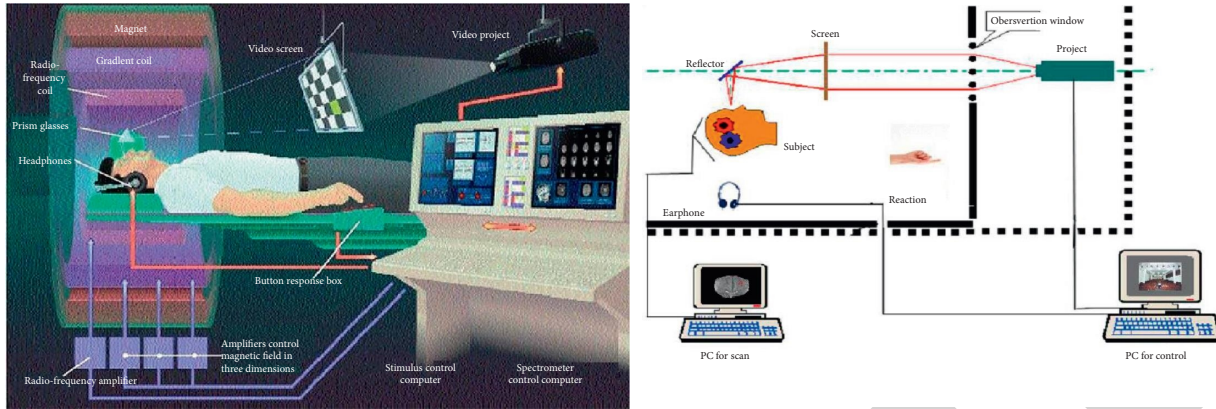


FIGURE 1: Study procedure.

the frontocentral midline electrode. Impedance for the electrodes was kept below 5 k Ω by using the electrode paste. The EEG signals were digitally sampled at 5000 Hz.

Next, the EEG data were analyzed by BrainVision Analyzer software (Brain Products GmbH, Gilching, Germany). First, scanner gradient artifacts and pulse-related artifacts were removed using an adaptive average subtraction method [20] and an algorithm based on a constrained independent component analysis (ICA) method [21]; meanwhile, the EEG signals were down-sampled at 250 Hz. Second, EEG signals, rereferenced to right and left mastoids (M1 M2), were low-pass filtered (between 0.01 and 35 Hz). Finally, eye blinks were manually detected and then regressed from the EEG signal.

The ERPs were computed for the target, novel, and standard stimuli, respectively. The P3a (novel effect) and P3b (target effect) components were separately defined as the largest positive deflection during the time window between -200 and 800 msec. The grand average ERP waveforms for the target and novel stimuli at typical three midline electrodes were all used to acquire our results in the study.

2.4. fMRI Acquisition and Analysis. fMRI data were acquired by a GE 3T MR scanner (GE Health Care, Milwaukee, WI) at the Department of Radiology of Xijing Hospital, Xi'an, China. The functional images were collected using a gradient-echo planar imaging sequence with the following parameters: TR = 2000 ms, TE = 30 ms, FOV = 240 mm * 240 mm, data matrix = 64 * 64, flip angle = 90', slices = 45, and 150 volumes. The anatomical images were also obtained (TR/TE: 8.2 ms/3.18 ms, field of view: 256 * 256 mm², matrix size: 512 * 512, flip angle = 9°, in-plane resolution: 0.5 * 0.5 mm², slice thickness = 1 mm, 196 sagittal slices).

Preprocessing and data analysis were both performed with the SPM8 software (Wellcome Department of Cognitive Neurology, London) implemented in MATLAB. First, in order to ensure the stability of the radial magnetic field, we discard the first four volumes of whole-brain images. Second, images were corrected for the acquisition delay between the slices and were realigned to the first volume. After the adjustment for movement-related effects, functional and

anatomical data were coregistered, spatially normalized into the standard stereotactic MNI space, and spatially smoothed with a 6 mm full width half maximum (FWHM) Gaussian kernel.

The event-related design (e-fMRI) was reported to be highly sensitive to the oddball task-related. A conventional analysis was conducted to assess the related activation in BOLD response associated with the processing of three stimuli. Each stimulus type (target, standard, and novel) was used as a regressor in the GLM after convolution with the hemodynamic response function. And the six movement parameters were used as regressors of noninterest. Target and novel functional activation was discriminated from baseline activation through the regression analysis. Regions that are significantly more activated by the targets relative to the novels were also given using a fixed-effect analysis ($p < 0.001$ uncorrected and the cluster size >50 voxels).

3. Results

3.1. Behavioral Data. Based on the statistical data, for the target stimuli in the task, all subjects responded correctly to 97.6% (SD: 5.7%) with a response time of 408 ms (SD: 48 ms), which indicated that they were able to concentrate on their tasks during the EEG recording and MRI scans.

3.2. ERP Data. Figure 2 shows the ERP results computed across 25 subjects for three electrodes (Fz, Cz, and Pz) and three stimuli (standard, target, and novel). The figure illustrates that P300 ERPs could be detected at the frontocentral (Fz), central (Cz), and centroparietal (Pz) electrodes for targets and novels. Using paired t -test, the novel-related P300 ERP (P3a) had a higher amplitude and decreased more slowly than the target-related P300 ERP (P3b), at Cz and Fz (all $p < 0.01$), but for Pz, the P3b ERP had a significantly higher amplitude ($p < 0.01$). P3a arose earlier than P3b at Cz and Fz (all $p < 0.01$), but the opposite phenomenon was observed for Pz ($p < 0.01$). Figure 2 demonstrates that P3a and P3b have distinct topographic amplitude distributions. The P3b activated frontal areas, while P3a activated frontoparietal areas. These topographic variations may be induced by different functional areas.

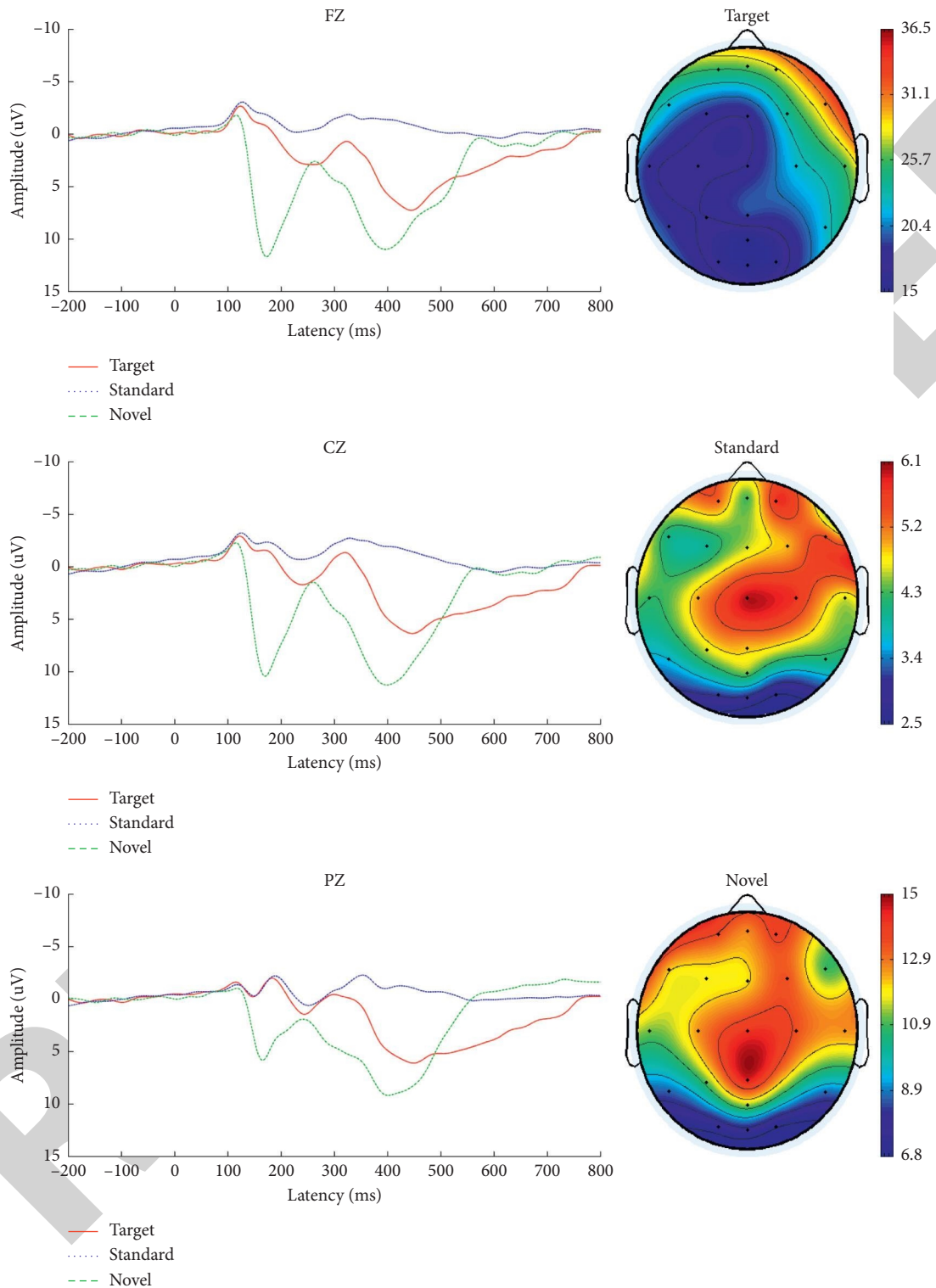


FIGURE 2: (a) Grand-averaged waveforms (mean across the 25 participants and 3 types of stimuli) on Pz, Cz, and Fz electrodes: target stimuli (red), standard (blue), and novels (green). (b) Topography distributions for the mean target (A), standard (B), and novel (C) amplitude.

3.3. *fMRI Data.* Figure 3(a) and Table 1 illustrate the activation for the novel stimuli. The novels activated the left frontoparietal areas, left precuneus areas, and the right insula. Figure 3(b) and Table 2 illustrate the activation for the target stimuli. The targets activated the bilateral fusiform gyrus, left frontal areas, and

bilateral insula. Figure 3(c) and Table 3 illustrate the activation for the novel-target contrast. These included the left frontoparietal areas, the left postcentral, and the left fusiform.

Gray reflects the background baseline state of the cerebral cortex; the darker the color, the closer to orange-red,

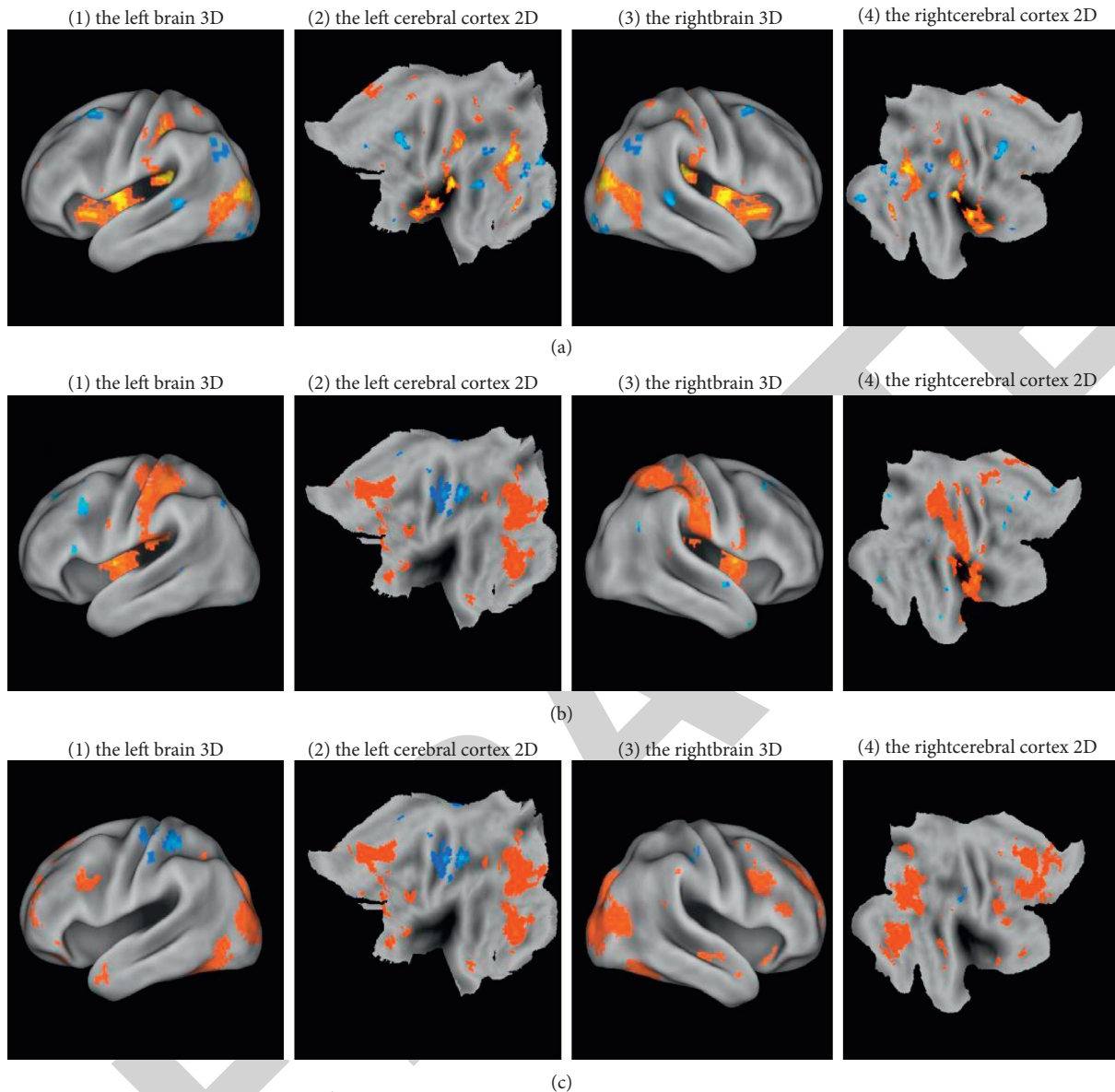


FIGURE 3: Functional activation 3D maps of left and right brain obtained for the novel (a), target (b), and target-novel contrast (c). (a) Brain regions showing activity to the novel stimuli. (b) Brain regions showing activity to the target stimuli. (c) Brain regions showing activity to the novel-target contrast. Reported activation became all thresholds at $p < 0.001$ uncorrected. Gray reflects the background baseline state of the cerebral cortex; the darker the color, the closer to orange-red, indicating that the increased rate of blood oxygen concentration in the brain area is more significant, indicating that the area is being activated. The lighter the color, the closer to blue, which means that the rate of decrease in blood oxygen concentration in this brain area is more significant, indicating that this area is negatively activated. a1: in the new heterostimulus task state, the activation area of the left brain 3D model; a2: in the new heterostimulus task state, the activation area of the 2D model of the left cerebral cortex; a3: in the new heterostimulus task state, the activation area of the right brain 3D model; a4: in the new heterostimulus task state, the activation area of the 2D model of the right cerebral cortex; b1: in the target stimulation task state, the activation area of the left brain 3D model; b2: in the target stimulation task state, the activation area of the 2D model of the left cerebral cortex expanded; b3: in the target stimulation task state, the activation area of the right brain 3D model; b4: in the target stimulation task state, the activation area of the 2D model of the right cerebral cortex; c1: for fMRI image data, using target stimulation-new stimulation, the activation area of the left brain 3D model; c2: for fMRI image data, using target stimulation-differential stimulation, the activation area of the 2D model of the left cerebral cortex; c3: for fMRI image data, use target stimulation-new stimulation, the activation area of the right brain 3D model; c4: for fMRI image data, using target stimulation-differential stimulation, the activation area of the 2D model of the right cerebral cortex.

TABLE 1: Regions of P300 FMRI activation to the novels.

Peak MNI coordinate	Anatomical area	K (cluster extent)	Peak Z score
-27 18 51	Frontal_Mid_L (aal)	107	5.0358
0 -60 36	Precuneus_L (aal)	69	4.1338
-39 -3 12	Insula_R (aal)	53	4.254
-51 -36 39	Parietal_Inf_L(aal)	57	4.0481

The coordinates x , y , and z (mm) are all given in the Montreal Neurological Institute (MNI) standard stereotactic space. The results are all significant at the voxel level $p < 0.001$ uncorrected and for the least cluster extent of 50 voxels. Overall z score: $z = (X-\mu)/\sigma$ where $X-\mu$ is the deviation from the mean and σ represents the standard deviation. Sample z score.

TABLE 2: Regions of P300 FMRI activation to the targets.

Peak MNI coordinate	Anatomical area	K (cluster extent)	Peak Z score
-27 -75 -9	Fusiform_L (aal)	162	4.6535
-48 21 21	Frontal_Inf_Tri_L (aal)	101	4.0602
-27 -27 54	Precentral_L (aal)	92	3.85
-36 12 54	Frontal_Mid_L (aal)	107	4.3317
14 -80 -8	Fusiform_R (aal)	147	4.7589
32 8 14	Insula_R (aal)	63	3.7151
-34 0 12	Insula_L (aal)	54	3.5945

The coordinates x , y , and z (mm) are all given in the Montreal Neurological Institute (MNI) standard stereotactic space. The results are all significant at the voxel level $p < 0.001$ uncorrected and for the least cluster extent of 50 voxels.

TABLE 3: Regions of P300 FMRI activation to novels-targets contrast.

Peak MNI coordinate	Anatomical area	K (cluster extent)	Peak Z score
-33 -48 -18	Fusiform_L (aal)	92	4.0206
-27 -45 72	Postcentral_L (aal)	212	4.1919
-24 -60 48	Parietal_Sup_L (aal)	69	3.5715
-51 33 21	Frontal_Inf_Tri_L (aal)	72	4.18

The coordinates x , y , and z (mm) are all given in the Montreal Neurological Institute (MNI) standard stereotactic space. The results are all significant at the voxel level $p < 0.001$ uncorrected and for the least cluster extent of 50 voxels.

indicating that the increased rate of blood oxygen concentration in the brain area is more significant, indicating that the area is being activated. The lighter the color, the closer to blue, which means that the rate of decrease in blood oxygen concentration in this brain area is more significant, indicating that this area is negatively activated.

4. Discussion

The current study used the simultaneous ERP/fMRI data collected in a visual three-stimulus oddball task to examine the differences of spatiotemporal neural dynamics between the P3a and P3b and the neuropsychological origins underlying these two ERPs.

The results obtained from the electrical recording, as shown in Figure 2, showed that P3a and P3b have different topographic amplitude distributions, which were in line with previous studies [29, 30]. As expected, two P300 ERPs were observed at middle sites (Fz, Cz, Pz, C3, and C4) for the novel and target conditions, and statistical differences in amplitudes between targets and novels were found [30, 31]. P3a and P3b data, using a difficult target/standard discrimination task in a three-stimulus paradigm from 120 healthy young adults, have shown that P3a has a central maximum, whereas P3b has a parietal maximum, and the

peak latency for both was shorter over the frontal and longer over the parietal sites [7, 19, 32].

Simultaneous fMRI and ERP findings demonstrated different brain regions related to different stimuli. P3a and P3b generation is assumed to stem from frontal and temporal/parietal activation. In the present study, P3a was related to the frontal lobe. It is proposed that P3a may be generated when rare or novel stimuli are processed if sufficient attentional focus is engaged (see Figure 3 and Tables 1–3) [33]. Many studies suggest that a frontal attention mechanism governs neural responsivity to novels [34] and then implies top-down control [35]. Attentional resources used to maintain memory items in parietal regions may result from response organization produced by bottom-up processing [7]. P3b was associated with parietal regions, prefrontal cortex, and medial temporal regions [36]. Evidence suggested that P3b appears when subsequent attentional resource activation promotes memory operations in temporal-parietal areas [37, 38]. Thus, the simultaneous ERP/fMRI findings extended the proposed model which suggested that P300 comprises an early attention process stemming from a frontal working memory representational change to produce the P3a, and the attention-driven stimulus signal is then transmitted to temporal and parietal structures, which were related to P3b [36, 39–41].

The limitations of this study should also be mentioned. First, 19 of the 25 subjects, from the Fourth Military Medical University, showed higher scores (128 ± 5) in the intelligence tests, which may have affected the result. The subsequent research can explore the potential impact of intelligence on ERP. Second, ERP analysis was restricted to only 3 electrodes without taking into account the full amount of the temporospatial information included in the ERP data. Third, gender has been shown to modulate the P300 component in emotional oddball tasks [42], but our sample included both female and male participants. Consequently, it is unknown whether our results were affected by the gender effect.

Furthermore, in order to better promote the fusion research of EEG-fMRI, there are still some deficiencies in the research of this article; the specific improvements are as follows.

Offline antialiasing processing is performed on the three artifact components of pulse artifact, gradient artifact, and electrocardiographic artifact. Due to the tedious experiment of synchronously collecting EEG signals in the magnetic resonance scanner, the limb movement or Mental state, etc. may introduce many unknown artifacts. Therefore, how to simplify the collection steps and minimize the generation of unknown artifacts is a problem to be improved in the future.

The amount of experimental calculation data of the synchronous EEG-fMRI brain-computer interface system in this article is large. In order to have a better real-time effect and reduce the amount of calculation, we only conducted the lead of the specific brain area where the P300 signal is active and analyze and ignore the information that other leads may reflect. Therefore, this topic should continue to improve the research. In addition, only 32-lead amplifiers were used in this experiment. In order to observe EEG signals more accurately, it may be considered to introduce 64-lead or 128-lead amplifiers for acquisition to obtain more detailed EEG information.

Because this experiment is designed for the P300 signal, but the research methods are universal, the next step should consider applying the synchronous EEG-fMRI brain-computer interface system to more experimental paradigms, such as emotion recognition and SSVEP.

Since this article only focuses on the EEG signals in the magnetic resonance scanning environment, most of the introduced artifacts are eliminated through real-time artifact removal processing. Therefore, in future research, the fMRI signal should be processed and the electroencephalogram signal and the fMRI signal should be fused to develop a brain signal that can observe multimodalities in real time, thus laying a foundation for humans to understand the brain from multiple angles and promote the development of brain science.

5. Conclusion

The integration of event-related potential (ERP) and functional magnetic resonance imaging (fMRI) can be used as a bridge between the well-established field of evoked cognitive potentials and the fast-growing field of fMRI. The simultaneous EEG/fMRI data provided further insight into

processes underlying the functional brain activation. In the oddball task, our results showed that P300 ERP induced by target stimulation and novel stimulation can be detected at the Fz, Cz, and Pz electrodes. At Cz and Fz, compared with P3b related to the target stimulus, the P3a related to the novel stimulus has a higher amplitude and the waveform declines more slowly. But at Pz, P3b has a higher amplitude than P3a. P3a appeared earlier than P3b at Cz and Fz, but the opposite phenomenon was observed at the Pz electrode. The activated brain regions of P3a included the left frontal-parietal lobe region, left anterior wedge lobe region, and right insula, while the target-driven P3b was significantly associated with BOLD changes in the bilateral fusiform gyrus, the left frontal region, and the bilateral insula. In summary, the current study replicates and extends prior studies.

Abbreviations

EEG:	Electroencephalogram
EEG-fMRI:	Simultaneous EEG and fMRI recordings
MRI:	Magnetic resonance imaging
BOLD:	Blood oxygen level-dependent
fMRI:	Functional magnetic resonance imaging
ERP:	Event-related potential
MNE:	Minimum norm estimate
ECD:	Equivalent current dipole
DCD:	Distributed current density
HRF:	Hemodynamic response function.

Data Availability

The data used to support the findings of this study are available from the corresponding author upon request.

Conflicts of Interest

The authors declare no conflicts of interest.

Acknowledgments

The authors are grateful to Professor Wei Qin for reading and correcting the manuscript and for fruitful criticisms. The authors thank Professor Junye Liu who designed and participated in the experiment in this study. Special thanks are due to Rui Zhao for her help in processing and interpreting the EEG data and Dian Dai and Xinxin Zhang for their help in the acquisition of fMRI data. This work was supported by the Department of Radiology of Xijing Hospital that provided the MRI device. This project was supported by the National Natural Science Foundation of China (Grant no. 61806210) and the National Social Science Foundation of China (Grant no. 15BSH023).

References

- [1] J. Polich, "Updating P300: an integrative theory of P3a and P3b," *Clinical Neurophysiology*, vol. 118, no. 10, pp. 2128–2148, 2007.
- [2] E. Donchin, "Surprise!? Surprise?" *Psychophysiology*, vol. 18, no. 5, pp. 493–513, 1981.

- [3] S. Adachi, K. Morikawa, and H. Nittono, "Event-related potentials elicited by unexpected visual stimuli after voluntary actions," *International Journal of Psychophysiology*, vol. 66, no. 3, pp. 238–243, 2007.
- [4] R. Johnson, "On the neural generators of the P300 component of the event-related potential," *Psychophysiology*, vol. 30, no. 1, pp. 90–97, 1993.
- [5] E. Snyder and S. A. Hillyard, "Long-latency evoked potentials to irrelevant, deviant stimuli," *Behavioral Biology*, vol. 16, no. 3, pp. 319–331, 1976.
- [6] N. K. Squires, K. C. Squires, and S. A. Hillyard, "Two varieties of long-latency positive waves evoked by unpredictable auditory stimuli in man," *Electroencephalography and Clinical Neurophysiology*, vol. 38, no. 4, pp. 387–401, 1975.
- [7] M. A. Conroy and J. Polich, "Normative variation of P3a and P3b from a large sample," *Journal of Psychophysiology*, vol. 21, no. 1, pp. 22–32, 2007.
- [8] H. Gaeta, D. Friedman, and G. Hunt, "Stimulus characteristics and task category dissociate the anterior and posterior aspects of the novelty P3," *Psychophysiology*, vol. 40, no. 2, pp. 198–208, 2003.
- [9] E. Yago, C. Escera, K. Alho, M. H. Giard, and J. M. Serra-Grabulosa, "Spatiotemporal dynamics of the auditory novelty-P3 event-related brain potential," *Cognitive Brain Research*, vol. 16, no. 3, pp. 383–390, 2003.
- [10] V. P. Clark, S. Fannon, S. Lai, and R. Benson, "Paradigm-dependent modulation of event-related fMRI activity evoked by the oddball task," *Human Brain Mapping*, vol. 14, no. 2, pp. 116–127, 2001.
- [11] J. R. Foucher, H. Otzenberger, and D. Gounot, "The BOLD response and the gamma oscillations respond differently than evoked potentials: an interleaved EEG-fMRI study," *BMC Neuroscience*, vol. 4, no. 1, p. 22, 2003.
- [12] J. R. Foucher, H. Otzenberger, and D. Gounot, "Where arousal meets attention: a simultaneous fMRI and EEG recording study," *Neuroimage*, vol. 22, no. 2, pp. 688–697, 2004.
- [13] K. A. Kiehl, K. R. Laurens, T. L. Duty, B. B. Forster, and P. F. Liddle, "Neural sources involved in auditory target detection and novelty processing: an event-related fMRI study," *Psychophysiology*, vol. 38, no. 1, pp. 133–142, 2001.
- [14] R. T. Knight, M. F. Grabowecy, and D. Scabini, "Role of human prefrontal cortex in attention control," *Advances in Neurology*, vol. 66, pp. 21–26, 1995.
- [15] Y. Li and W. Wang, "Source analysis of P3a and P3b components to investigate interaction of depression and anxiety in attentional systems," *Scientific Reports*, vol. 5, no. 1, Article ID 17138, 2015.
- [16] R. Verleger, P. Jas'kowskis, and E. Wascher, "Evidence for an integrative role of P3b in linking reaction to perception," *Journal of Psychophysiology*, vol. 19, p. 150, 2005.
- [17] S. Yamaguchi and R. T. Knight, "Effects of temporal-parietal lesions on the somatosensory P3 to lower limb stimulation," *Electroencephalography and Clinical Neurophysiology/ Evoked Potentials Section*, vol. 84, no. 2, pp. 139–148, 1992.
- [18] J. Polich and M. D. Comerchero, "P3a from visual stimuli: typicality, task, and topography," *Brain Topography*, vol. 15, no. 3, pp. 141–152, 2003.
- [19] M. Soltani and R. T. Knight, "Neural origins of the P300," *Critical Reviews in Neurobiology*, vol. 14, pp. 199–224, 2000.
- [20] P. J. Allen, O. Josephs, and R. Turner, "A method for removing imaging artifact from continuous EEG recorded during functional MRI," *NeuroImage*, vol. 12, no. 2, pp. 230–239, 2000.
- [21] Y. Leclercq, J. Schrouff, Q. Noirhomme, P. Maquet, and C. Philipps, "fMRI artefact rejection and sleep scoring toolbox," *Computational Intelligence and Neuroscience*, vol. 2011, p. 11, Article ID 598206, 2011.
- [22] A. Gazzaley and A. C. Nobre, "Top-down modulation: bridging selective attention and working memory," *Trends in Cognitive Sciences*, vol. 16, no. 2, pp. 129–135, 2012.
- [23] S. Kastner, P. de Weerd, and L. G. Ungerleider, "Texture segregation in the human visual cortex: a functional MRI study," *Journal of Neurophysiology*, vol. 83, no. 4, pp. 2453–2457, 2000.
- [24] J. R. Doherty, A. Rao, M. M. Mesulam, and A. C. Nobre, "Synergistic effect of combined temporal and spatial expectations on visual attention," *The Journal of neuroscience: the official journal of the Society for Neuroscience*, vol. 25, no. 36, pp. 8259–8266, 2005.
- [25] I. C. Griffin, C. Miniussi, and A. C. Nobre, "Multiple mechanisms of selective attention: differential modulation of stimulus processing by attention to space or time," *Neuropsychologia*, vol. 40, no. 13, pp. 2325–2340, 2002.
- [26] A. Correa, J. Lupiáñez, E. Madrid, and P. Tudela, "Temporal attention enhances early visual processing: a review and new evidence from event-related potentials," *Brain Research*, vol. 1076, no. 1, pp. 116–128, 2006.
- [27] J. T. Coull and A. C. Nobre, "Where and when to pay attention: the neural systems for directing attention to spatial locations and to time intervals as revealed by both PET and fMRI," *Journal of Neuroscience*, vol. 18, no. 18, pp. 7426–7435, 1998.
- [28] J. Rimmelme, E. Sussman, and H. Jolsvai, "Auditory target detection is affected by implicit temporal and spatial expectations," *Journal of Cognitive Neuroscience*, vol. 23, no. 5, pp. 1136–1147, 2010.
- [29] J. Polich, "P300 in clinical applications," in *Electroencephalography: Basic Principles, Clinical Applications and Related Fields*, E. Niedermeyer and F. Lopes Da Silva, Eds., pp. 1073–1091, Williams & Wilkins, Baltimore, MD, USA, 1999.
- [30] H. Otzenberger, D. Gounot, and J. R. Foucher, "P300 recordings during event-related fMRI: a feasibility study," *Cognitive Brain Research*, vol. 23, no. 2–3, pp. 306–315, 2005.
- [31] T. Eichele, K. Specht, M. Moosmann et al., "Assessing the spatiotemporal evolution of neuronal activation with single-trial event-related potentials and functional MRI," *Proceedings of the National Academy of Sciences*, vol. 102, no. 49, pp. 17798–17803, 2005.
- [32] D. Linden, "The P300: where in the brain is it produced and what does it tell us?" *Neuroscientist*, vol. 5, no. 6, pp. 563–76, 2003.
- [33] M. Brázdil, R. Roman, P. Daniel, I. Rektor, and I. Rektor, "Intracerebral somatosensory event-related potentials: effect of response type (button pressing versus mental counting) on P3-like potentials within the human brain," *Clinical neurophysiology: official journal of the International Federation of Clinical Neurophysiology*, vol. 114, no. 8, pp. 1489–96, 2003.
- [34] S. Suwazono, L. Machado, and R. T. Knight, "Predictive value of novel stimuli modifies visual event-related potentials and behavior," *Clinical Neurophysiology*, vol. 111, no. 1, pp. 29–39, 2000.
- [35] C. Bledowski, D. Prvulovic, R. Goebel, F. E. Zanella, and D. E. J. Linden, "Attentional systems in target and distractor processing: a combined ERP and fMRI study," *Neuroimage*, vol. 22, no. 2, pp. 530–540, 2004.

- [36] J. K. Wynn, A. M. Jimenez, B. J. Roach et al., "Impaired target detection in schizophrenia and the ventral attentional network: findings from a joint event-related potential-functional MRI analysis," *NeuroImage: Clinical*, vol. 9, pp. 95–102, 2015.
- [37] M. Brazdil, I. Rektor, P. Daniel, M. Dufek, and P. Jurak, "Intracerebral eventrelated potentials to subthreshold target stimuli," *Clin Neurophysiol*, vol. 112, pp. 650–61, 2001.
- [38] L. Squire and E. Kandel, *Memory From Mind to Molecules*, Scientific American Library, New York, NY, USA, 1999.
- [39] K. A. Kiehl, M. C. Stevens, K. R. Laurens, G. Pearlson, V. D. Calhoun, and P. F. Liddle, "An adaptive reflexive processing model of neurocognitive function: supporting evidence from a large scale (n=100) fMRI study of an auditory oddball task," *Neuroimage*, vol. 25, no. 3, pp. 899–915, 2005.
- [40] S. Campanella, M. Bourguignon, P. Peigneux et al., "BOLD response to deviant face detection informed by P300 event-related potential parameters: A simultaneous ERP-fMRI study," *NeuroImage*, vol. 71, pp. 92–103, 2013.
- [41] S. G. Horowitz, "Correlations and dissociations between BOLD signal and P300 amplitude in an auditory oddball task: a parametric approach to combining fMRI and ERP," *Magnetic Resonance Imaging*, vol. 20, pp. 319–325, 2001.
- [42] S. Campanella, L. Falbo, M. Rossignol et al., "Sex differences on emotional processing are modulated by subclinical levels of alexithymia and depression: A preliminary assessment using event-related potentials," *Psychiatry Research*, vol. 197, no. 1-2, pp. 145–153, 2012.